CHAPTER 21

Capillarity

21.1 CAPILLARY PRESSURE

One of the most common fluid mechanical effects exploited in microfluidics is *capillarity*, *e.g.*, induced fluid motion in very small channels. As we have seen, curved surfaces introduce a pressure gradient that can be exploited in order to drive fluids. In Eq. 20.11, we can see that for small radii, this pressure drop can amount to significant values.

This is exploited by using channels with very small diameters; in the simplest case a circular capillary is used (see Fig. 21.1a). From Eq. 20.11, we can deduce that for a circular tube for which $r_1 = r_2 = r$, the pressure difference is given as

$$p_{\text{inside}} - p_{\text{outside}} = \frac{2\,\gamma}{r} \qquad \text{(Eq. 21.1)}$$

From geometry it follows that

$$\frac{d_c}{2} = \cos\Theta\, r$$

Therefore, Eq. 21.1 can be rewritten as

$$p_{\text{inside}} - p_{\text{outside}} = \frac{4\,\gamma\,\cos\Theta}{d_c} \qquad \text{(Eq. 21.2)}$$

Eq. 21.2 expresses the capillary pressure drop across the curved surface in a thin capillary. The pressure drop is positive, *i.e.*, the pressure inside the liquid column is higher than in the ambiance. Therefore the capillary will pull the liquid up. This driving pressure is often referred to as the *capillary pressure*.

The rising liquid column will experience gravitational forces that eventually balance the capillary forces. At this equilibrium, the column will have reached a total height of h_c, which can be derived as

$$\begin{aligned}
(p_{\text{inside}} - p_{\text{outside}})\; A &= \rho\, g\, A\, h_c \\
\frac{4\,\gamma\,\cos\Theta}{d_c} &= \rho\, g\, h_c \\
h_c &= \frac{4\,\gamma\,\cos\Theta}{d_c\,\rho\, g} && \text{(Eq. 21.3)} \\
&= \frac{4\,\cos\Theta}{d}\, L_c^2 && \text{(Eq. 21.4)}
\end{aligned}$$

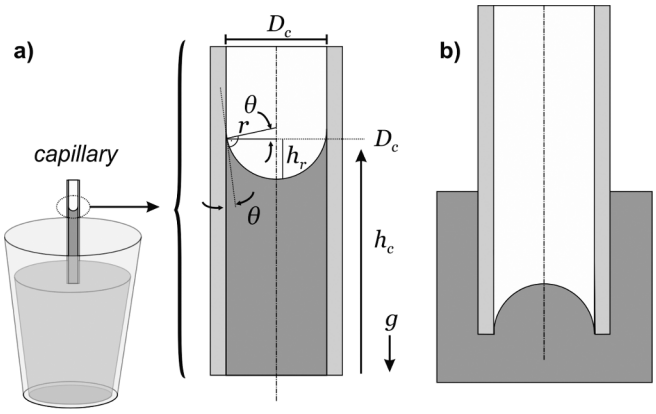

Fig. 21.1 *a) Capillary pressure that pulls a liquid into a thin capillary. b) An example of negative capillary pressure.*

The parameter h_c is often referred to as *capillary height* or *Jurin*[1] *height* named after English physician James Jurin. However, there are several accounts of earlier studies on capillarity, including work by Leonardo da Vinci in the 15$^{\text{th}}$ century and even work by Greek mathematician and engineer Hero of Alexandria who used capillarity in a number of setups more than 2000 years ago [2].

Please note that in Eq. 21.4, we introduced a parameter that is referred to as the *capillary length* L_c, which we will briefly introduce.

21.2 CAPILLARY LENGTH

The *capillary length* L_c is an important number that we will use in the following sections. As we will see, numerous fluid mechanical phenomena originating from the effects of surface tension are dependent on this parameter. For a given liquid, it is sometimes also referred to as *capillary constant* and defined as

$$L_c = \sqrt{\frac{\gamma}{\rho\, g}} \qquad [\text{m}] \qquad \text{(Eq. 21.5)}$$

This number is a constant for a given liquid. As we can see in Eq. 21.4, the introduction of this constant makes the equation independent of the fluid in question. This means that the capillary height can be given normalized to L_c, which makes it valid for every fluid. We will see that there are a number of occasions where this constant can be used for a given fluid mechanical phenomenon thus making the derived equations valid for all fluids by multiplying it with the capillary length.

Analytically, the capillary length puts the surface tension forces in relation with the inertia forces. As stated, it can be calculated for any given fluid. It can also be calculated for fluid immersed in a different fluid, in which case the difference in densities and the interfacial surface tension have to be used in Eq. 21.5. Using water in air as the two fluids and standard conditions, the capillary length is calculated to be $L_c = 2.71\,\text{mm}$. For a droplet, the capillary length indicates that for all droplets with diameters in the range of 2.71 mm, the effects of gravity can be ignored. This is an interesting consideration, *e.g.*, for rain drops (which rarely are more than a millimeter in diameter). Although often drawn in tear-shaped form, raindrops will always be near-perfect spheres.

21.2.1 Normalized Capillary Heights

Using the capillary length, the capillary heights of tubes with different diameters can be calculated in Eq. 21.4. The results are depicted in Fig. 21.2. Fig. 21.2a shows the capillary height h_c normalized to L_c^2. The values shown are calculated for different wall contact angles Θ starting with $\Theta = 0°$ (perfectly wetting) as the topmost curve all the way down to $\Theta = 180°$ (perfectly non-wetting) in increments of 20°. For $\Theta = 90°$, the line is horizontal.

a) *Normalized capillary height.*

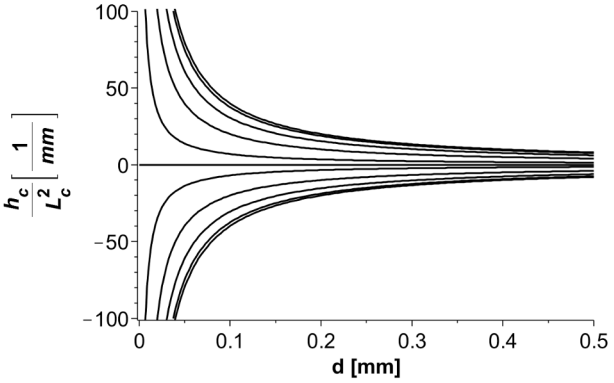

b) *Capillary heights calculated for water at STP conditions.*

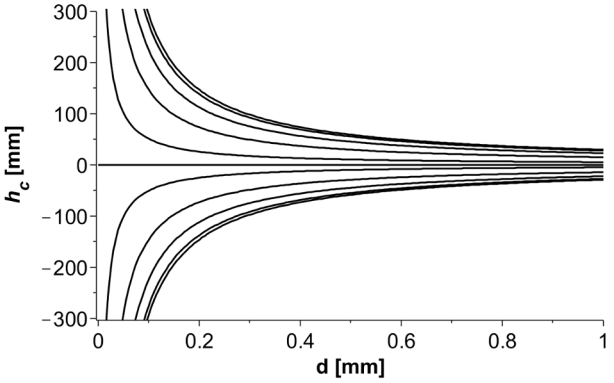

Fig. 21.2 *Calculated capillary height values h_c for different capillary diameters d. The curves displayed are for $\Theta = 0°$ (topmost) to $\Theta = 180°$ (lowermost) in increments of 20°. The horizontal line is obtained for $\Theta = 90°$.*

[1] James Jurin was an English physician who did important studies in capillary motion [1].

The calculated values are valid for any fluid and depend only on the wall contact angle Θ of this fluid. Fig. 21.2b shows the capillary height h_c for water, again calculated for the different wetting cases.

21.2.2 Negative Capillary Pressure

One interesting aspect can be seen in Eq. 21.3 and Fig. 21.2: for contact angles of $\Theta > 90°$, the capillary pressure and the capillary height are negative (see Fig. 21.1b). For these cases, the capillary will represent a pressure barrier, *i.e.*, an overpressure is required to push the liquid into the capillary. This is the case, *e.g.*, when pumping aqueous solutions through hydrophobic capillaries made from polytetrafluoroethylene, for example.

21.2.3 Meniscus Depth

We will discuss the fluid mechanics of the meniscus in section 21.3. However, for small capillary diameters, this meniscus can be adequately approximated by a circle (see Fig. 21.1). The depth of the meniscus h_r can be calculated by using the following geometrical relations

$$\cos\theta\, r = \frac{d}{2} \tag{Eq. 21.6}$$

$$\sin\theta\, r = r - h_r \rightarrow h_r = r\,(1 - \sin\theta) \tag{Eq. 21.7}$$

Inserting Eq. 21.7 into Eq. 21.6 results in

$$h_r = \frac{d}{2}\,\frac{1-\sin\theta}{\cos\theta} \tag{Eq. 21.8}$$

21.2.4 Capillary Number

The relevant dimensionless quantity to assess the influence of the capillary forces compared to the viscous forces of the fluid is the *capillary number* Ca (see section 9.9.10). In strongly porous materials, the capillary number is usually in the range of $\mathrm{Ca} < 1 \times 10^{-5}$, in which case the viscous forces of the fluid can be ignored, and the flow is purely driven by capillary forces. Driving microfluidic flows with capillarity is one of the oldest and still most commonly used ways of controlling fluid motion.

21.3 MENISCUS FORMATION

Capillarity is the reason why a liquid forms meniscus at the wall of a vessel (see Fig. 21.3). In the following section, we will derive the equations that describe the curvature of the surface in close proximity of the wall. As

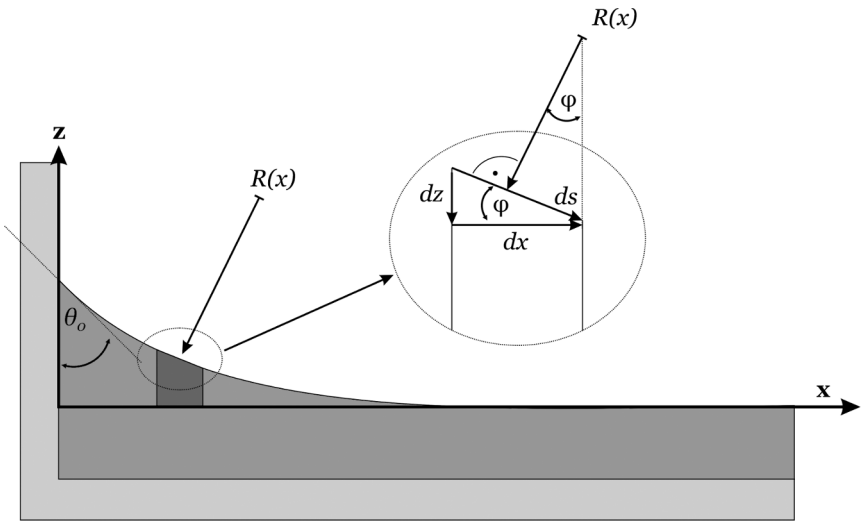

Fig. 21.3 *Meniscus formation at the wall of a vessel.*

we will see, there is one (surprisingly) easy way of deriving the curvature, which, however, yields (surprisingly) incorrect results. The second approach we will take allows deriving the curvature implicitly. This approach yields correct results.

21.3.1 Derivation Using the Surface Curvature

The first approach we will take is based on the curvature of the surface because of the Young-Laplace pressure drop across the curved interface. The shape of the meniscus is due to the balance of forces from gravitation and the Young-Laplace pressure drop at the curved surface. For a fluid segment dx, the force balance is

$$\begin{aligned} p_{\text{gravity}} &= p_{\text{Young-Laplace}} \\ \frac{d\left(m\,g\right)}{dA} &= \frac{\gamma}{R\left(x\right)} \\ \frac{\rho\,g\,dV}{dA} &= \gamma\,\frac{d^2z\left(x\right)}{dx^2} \\ \rho\,g\,z\left(x\right) &= \gamma\,\frac{d^2z\left(x\right)}{dx^2} \\ \frac{\rho\,g}{\gamma}\,z\left(x\right) &= \frac{d^2z\left(x\right)}{dx^2} \end{aligned} \qquad \text{(Eq. 21.9)}$$

where we used Eq. 3.103 to approximate the curvature. Noted that this equation is valid only if the changes in curvature $\frac{d^2z}{dx^2} = \frac{d}{dx}\left(\frac{dz}{dx}\right)$ are small because the function is a linearization of Eq. 3.102. As we will see, this approximation is incorrect, especially in close proximity to the wall where the meniscus is strongly curved. However, using the full equation of the surface curvature results in a differential equation that can only be solved numerically.

Eq. 21.9 is an ordinary second order differential equation with constant coefficients (see section 8.2.3), which is solved by a function of type

$$z\left(x\right) = c_1\,\mathrm{e}^{\sqrt{\frac{\rho\,g}{\gamma}}\,x} + c_2\,\mathrm{e}^{-\sqrt{\frac{\rho\,g}{\gamma}}\,x} \qquad \text{(Eq. 21.10)}$$

The details of this solution can be found in section 8.2.3.6. We see that the surface smooths out the farther we move away from the vessel wall; therefore $z\left(x\right) \to 0$ for $x \to \infty$, in which case we find that $c_1 = 0$. The second integration constant is found for the boundary condition at $x = 0$ where $\frac{dz}{dx} = -\frac{1}{\tan(\Theta_0)}$ because $\frac{dx}{dz} = -\tan\left(\Theta_0\right)$ at $x = 0$. Therefore we find

$$\begin{aligned} \frac{dz\left(x=0\right)}{dx} = -c_2\,\sqrt{\frac{\rho\,g}{\gamma}} &= -\frac{1}{\tan\left(\Theta_0\right)} \\ c_2 &= \frac{1}{\tan\left(\Theta_0\right)\,\sqrt{\frac{\rho\,g}{\gamma}}} \end{aligned}$$

which leads to the final solution

$$z\left(x\right) = \frac{1}{\tan\left(\Theta_0\right)\,\sqrt{\frac{\rho\,g}{\gamma}}}\,\mathrm{e}^{-\sqrt{\frac{\rho\,g}{\gamma}}\,x} \qquad \text{(Eq. 21.11)}$$

$$z\left(x\right) = \frac{L_c}{\tan\left(\Theta_0\right)}\,\mathrm{e}^{-\frac{x}{L_c}} \qquad \text{(Eq. 21.12)}$$

The meniscus therefore decays exponentially. In Eq. 21.12 we used the capillary length (see Eq. 21.5), which is characteristic length scale for the decay.

As already stated, this result is a crude approximation because the meniscus near the wall is strongly curved, which is in contradiction to our initial assumption of a not-strongly curved meniscus. This becomes especially obvious for liquid that wets the vessel wall well. For $\Theta_0 \to \frac{\pi}{2}$ (perfect wetting) Eq. 21.12 will converge to infinity, which is (obviously) incorrect.

21.3.2 Derivation Without Linearization

In order to find the correct solution, we need to apply the surface curvature without linearizing it. As already stated, this results in a nonlinear ordinary differential equation that is extremely difficult to solve analytically.

However, there are a couple of ways of solving this problem. Looking at Fig. 21.3, we first note the following relations

$$dx = \cos\varphi\, ds \tag{Eq. 21.13}$$

$$dz = -\sin\varphi\, ds \tag{Eq. 21.14}$$

$$ds = d\varphi\, R \qquad \rightarrow \frac{1}{R} = \frac{d\varphi}{ds} \tag{Eq. 21.15}$$

Using Eq. 21.15, we can rewrite Eq. 21.9 to

$$\frac{\rho\, g}{\gamma}\, z = \frac{d\varphi}{ds}$$

$$\frac{1}{L_c^2}\, z = \frac{d\varphi}{ds}$$

this time applying the nonlinearized form $\frac{d\varphi}{ds}$ to express the surface curvature. We now take the derivative with respect to s and apply Eq. 21.14

$$\frac{1}{L_c^2}\frac{dz}{ds} = \frac{d^2\varphi}{ds^2}$$

$$\frac{1}{L_c^2}\sin\varphi = \frac{d^2\varphi}{ds^2} \tag{Eq. 21.16}$$

We now apply a small trick in order to convert the double integral $\frac{d^2\varphi}{ds^2}$ to a single integral (see section 3.3.2) by exploiting the fact that

$$\frac{d^2\varphi}{ds^2}\frac{d\varphi}{ds} = \frac{d}{ds}\left(\frac{1}{2}\frac{d\varphi}{ds}^2\right)$$

which we can employ after multiplying Eq. 21.16 by $\frac{d\varphi}{ds}$

$$\frac{1}{L_c^2}\sin\varphi\frac{d\varphi}{ds} = \frac{d^2\varphi}{ds^2}\frac{d\varphi}{ds}$$

$$\frac{1}{L_c^2}\sin\varphi\frac{d\varphi}{ds} = \frac{d}{ds}\left(\frac{1}{2}\frac{d\varphi}{ds}^2\right)$$

$$\frac{1}{L_c^2}\sin\varphi\, d\varphi = d\left(\frac{1}{2}\frac{d\varphi}{ds}^2\right) \tag{Eq. 21.17}$$

Eq. 21.17 can be integrated to result in

$$-\frac{1}{L_c^2}\cos\varphi + c_1 = \frac{1}{2}\frac{d\varphi}{ds}^2 \tag{Eq. 21.18}$$

The integration constant is determined by the fact that for $\varphi \rightarrow 0$: $\frac{d\varphi}{ds} = 0$, in which case $c_1 = L_c$, which results in

$$\frac{2}{L_c^2}(1-\cos\varphi) = \frac{d\varphi}{ds}^2$$

$$\pm\frac{\sqrt{2}}{L_c}\sqrt{2\frac{1-\cos\varphi}{2}} = \frac{d\varphi}{ds}$$

Here we can exploit the fact that $\pm\sqrt{\frac{1-\cos\varphi}{2}} = \sin\frac{\varphi}{2}$ (see Eq. 3.35), which results in

$$\frac{2}{L_c}\sin\frac{\varphi}{2} = \frac{d\varphi}{ds} \tag{Eq. 21.19}$$

Eq. 21.19 contains the implicit solution to the contour of the meniscus. It is expressed as a function of the angle φ and the path variable s. As we will see, it is analytically possible but very tedious to derive the function $z(x)$ from Eq. 21.19. It is significantly easier to derive two functions from it, *i.e.*, $x(\varphi)$ and $z(\varphi)$. Using these

two equations, it is possible to calculate the contour implicitly by finding x and y as functions of the angle φ. The value range for φ is given by the initial contact angle $\varphi_0 = \frac{\pi}{2} - \Theta_0$ and $\varphi \to 0$ for $x \to \infty$.

Deriving $x(\varphi)$. We will start by deriving $x(\varphi)$. For this we replace ds in Eq. 21.19 using Eq. 21.13, resulting in

$$\frac{2}{L_c}\, dx = \frac{\cos\varphi}{\sin\frac{\varphi}{2}}\, d\varphi$$

which can be integrated to result in

$$\frac{2}{L_c}x + c_2 = 4\,\cos\frac{\varphi}{2} + 2\,\ln\left(\frac{1}{\sin\frac{\varphi}{2}} - \frac{1}{\tan\frac{\varphi}{2}}\right) \qquad \text{(Eq. 21.20)}$$

The integral is not straightforward, and it is best to locate it in a suitable integral table or by using, *e.g.*, *Maple*. The integration constant c_2 can be found for $x = 0$: $\varphi = \varphi_0$, in which case we find

$$c_2 = 4\,\cos\frac{\varphi_0}{2} + 2\,\ln\left(\frac{1}{\sin\frac{\varphi_0}{2}} - \frac{1}{\tan\frac{\varphi_0}{2}}\right)$$

This allows us to rewrite Eq. 21.19 as

$$\begin{aligned}
\frac{2}{L_c}x &= 4\,\cos\frac{\varphi}{2} + 2\,\ln\left(\frac{1}{\sin\frac{\varphi}{2}} - \frac{1}{\tan\frac{\varphi}{2}}\right) - \left(4\,\cos\frac{\varphi_0}{2} + 2\,\ln\left(\frac{1}{\sin\frac{\varphi_0}{2}} - \frac{1}{\tan\frac{\varphi_0}{2}}\right)\right)\\
\frac{1}{L_c}x &= 2\,\cos\frac{\varphi}{2} + \ln\left(\frac{1}{\sin\frac{\varphi}{2}} - \frac{1}{\tan\frac{\varphi}{2}}\right) - \left(2\,\cos\frac{\varphi_0}{2} + \ln\left(\frac{1}{\sin\frac{\varphi_0}{2}} - \frac{1}{\tan\frac{\varphi_0}{2}}\right)\right)\\
x &= L_c\left(2\,\cos\frac{\varphi}{2} + \ln\left(\frac{1}{\sin\frac{\varphi}{2}} - \frac{1}{\tan\frac{\varphi}{2}}\right) - \left(2\,\cos\frac{\varphi_0}{2} + \ln\left(\frac{1}{\sin\frac{\varphi_0}{2}} - \frac{1}{\tan\frac{\varphi_0}{2}}\right)\right)\right) \qquad \text{(Eq. 21.21)}
\end{aligned}$$

Eq. 21.21 allows us to find the values for x for a given angle φ.

Deriving $z(\varphi)$. We now turn to finding the function $z(\varphi)$, which can be derived by replacing ds in Eq. 21.19 using Eq. 21.14, resulting in

$$\frac{2}{L_c}\, dz = \frac{\sin\varphi}{\sin\frac{\varphi}{2}}\, d\varphi$$

which can be integrated as

$$\begin{aligned}
\frac{2}{L_c}z &= 4\,\sin\frac{\varphi}{2}\\
z &= 2\sqrt{L_c}\,\sin\frac{\varphi}{2} \qquad \text{(Eq. 21.22)}
\end{aligned}$$

Again, the integral $\frac{\sin\varphi}{\sin\frac{\varphi}{2}}\, d\varphi$ is best located in an integration table or by using an algebra tool. Eq. 21.22 is the sought equation. We now have two equations to calculate the values $x(\varphi)$ and $z(\varphi)$ and thereby implicitly find the meniscus contour.

21.3.3 Meniscus Contours

One important aspect that we can already see when looking at Eq. 21.21 and Eq. 21.22 is that they are both scaled to the capillary length L_c. Therefore the derived equations are correct for all liquids, irrespective of their physical properties because for each liquid, the capillary length is a constant. Therefore it is not necessary to calculate the meniscus shape for different liquids. If the wetting contact angle Θ_0 at the wall is known, the profile can be derived from Eq. 21.21 and Eq. 21.22.

Fig. 21.4 shows the calculated profiles for the meniscus at different wetting angles at the wall, starting from $\Theta_0 = 0°$ (perfectly wetting) as the topmost profile all the way to $\Theta_0 = 180°$ (perfectly non-wetting) as the bottommost profile in increments of 20°. Please note that Eq. 21.21 is discontinuous for $\Theta_0 = 90°$, which is why this profile is not shown. However, for $\Theta_0 = 90°$, there is no meniscus formation, and the surface remains flat. Fig. 21.4a shows the calculated meniscus shapes for water at STP conditions. As stated, the profiles will look identical for all liquids as long as Θ_0 is known. Fig. 21.4b shows this general meniscus shape normalized to the capillary length, the latter of course being different for different liquids.

a) *Meniscus for water at STP conditions*

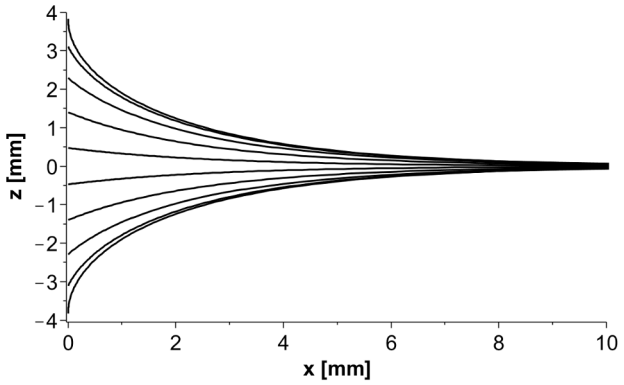

b) *Normalized meniscus*

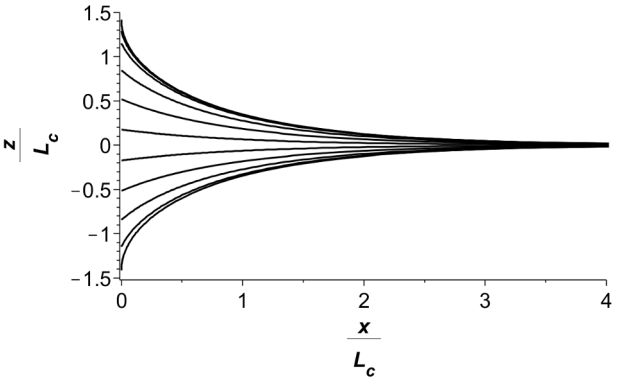

Fig. 21.4 *Calculated meniscus shape for water at STP conditions and for a normalized meniscus shape. The calculated profiles are for* $\Theta_0 = 0°$ *(perfectly wetting, topmost profile) in increments of 20° up to* $\Theta_0 = 180°$ *(perfectly non-wetting, bottommost profile). For* $\Theta_0 = 90°$*, the profile is flat (not shown).*

21.4 SUMMARY

In this section we discussed the concept of capillarity, which is a direct consequence of the surface tension of fluids. Capillarity is a major driving mechanism for microfluidic flows and is well known, *e.g.*, from the fact that a capillary of a hydrophilic material (such as glass) as well as a substrate with inherent porosity (such as a natural fiber) will transport fluids due to the fact that water wets them. Capillarity is one of the easiest functional mechanism to use in order to drive a microfluidic system and numerous platforms, *e.g.*, the lateral flow devices make ample use of this fact. We discussed the equations from which we can derive the capillary pressure as well as the capillary heights. We also detailed the shape of the liquid meniscus.

REFERENCES

[1] J. Jurin. "De Motu Aquarum Fluentium." In: *Philosophical Transactions*, vol. 30, no. 351-363 (1717), pp. 748–766 (cit. on p. 446).

[2] B. Woodcroft. *The pneumatics of Hero of Alexandria*. Vol. 1. Taylor Walton and Maberly London, 1851 (cit. on p. 446).